SUPPLEMENTAL FIGURES

Figure S1

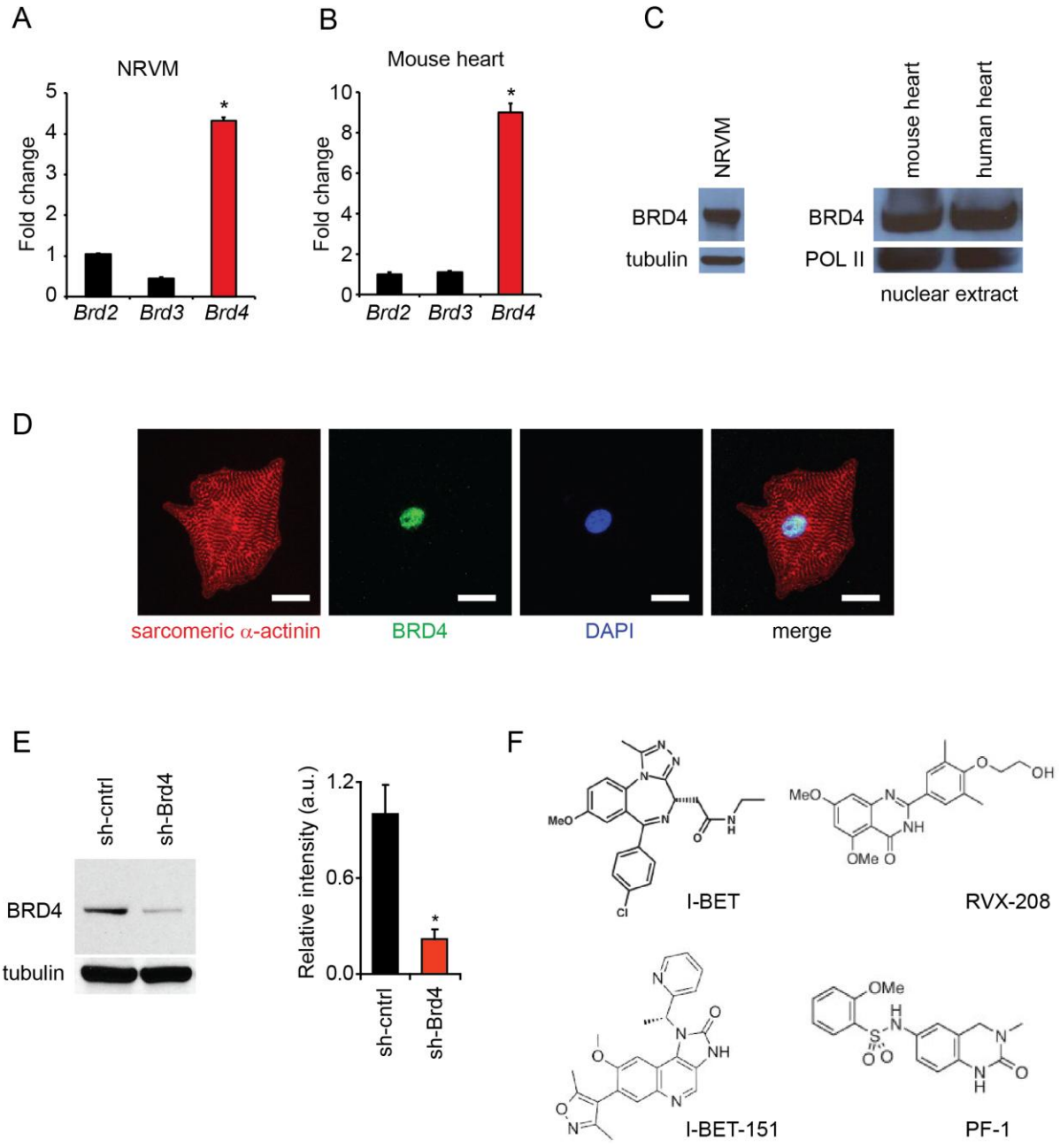

Figure S1 (related to Figure 1). BET expression in the heart. (A) Relative expression of indicated BET genes by qRT-PCR in (A) NRVM and (B) adult mouse heart tissue (N=4). P<0.05 vs. *Brd2* and *Brd3*. (C) Western blot demonstrating presence of BRD4 in NRVM whole cell extracts (left) and in adult mouse and human heart tissue nuclear protein extracts (right). Tubulin and RNA Pol II shown for loading. (D) Immunofluorescence staining in NRVM for BRD4 (green), α-actinin (red), DAPI (blue). Merged image demonstrates nuclear localized BRD4 signal. White bar=10 μM. (E) Western blot demonstrating effective knockdown of BRD4 protein in NRVM with densitometric quantification (N=3). *P<0.05 vs. sh-cntrl. (F) Chemical structures of BET inhibitors used in Figure 1F. Data shown as mean $\pm$ SEM.

Figure S2

A

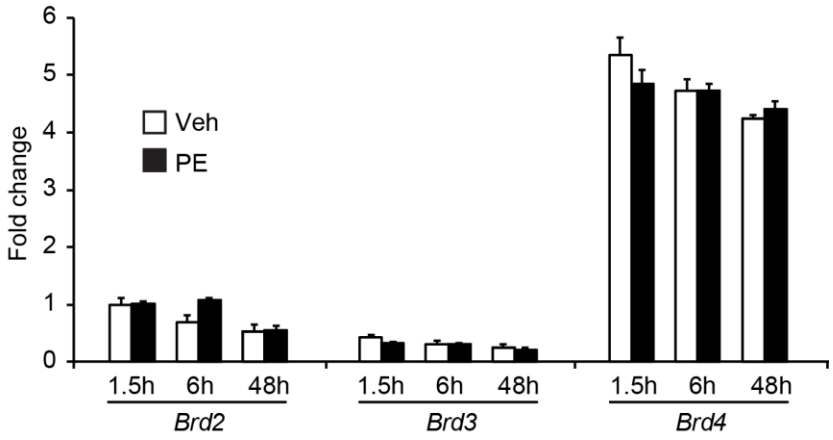

Figure S2 (related to Figure 2). BET expression in NRVM is invariant with PE stimulation. (A) Relative expression of *Brd2-4* genes by qRT-PCR in NRVM treated with PE (100 μM) for indicated time-points (N=4). Data shown as mean ± SEM.

Figure S3

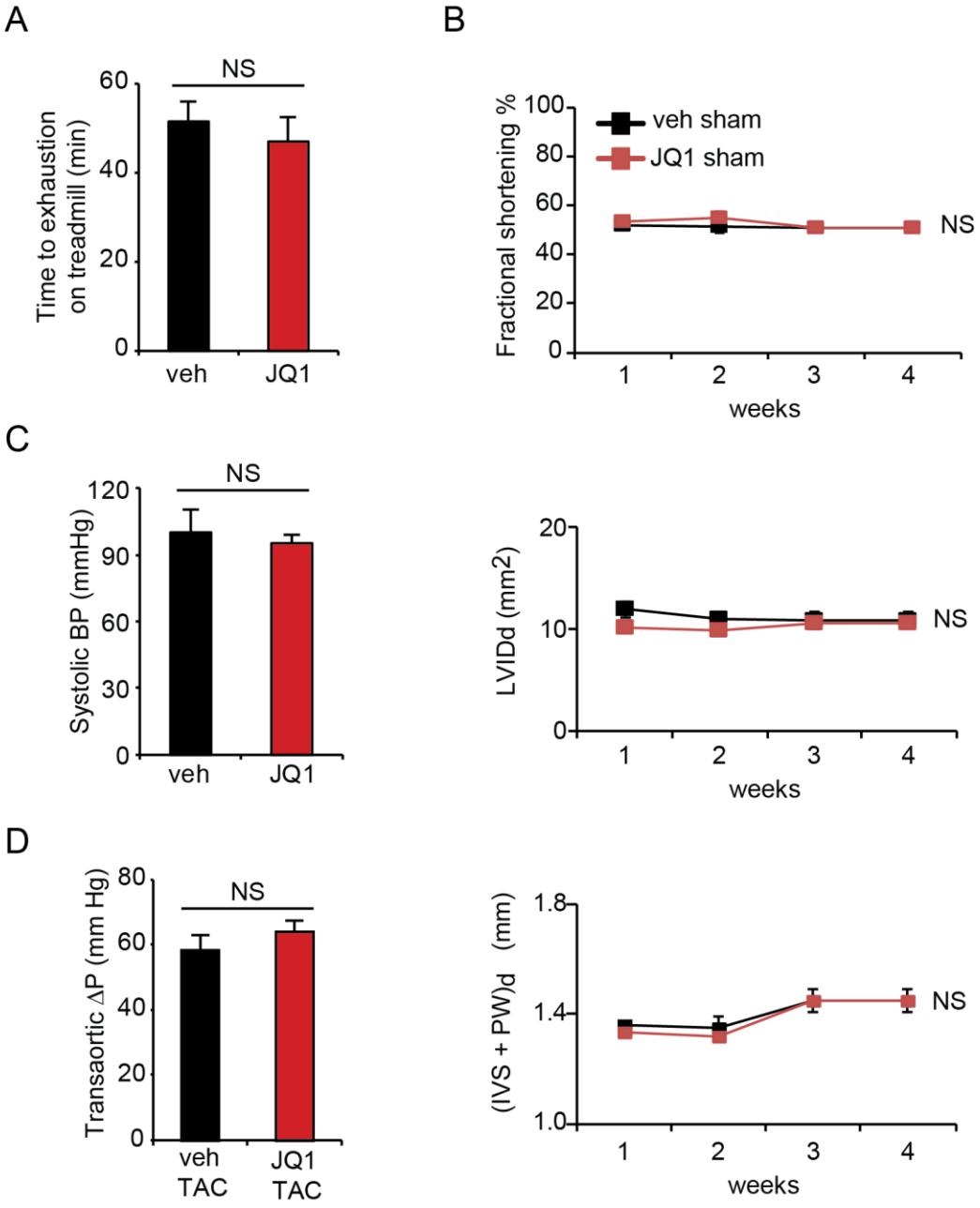
A
NS
Time to exhaustion on treadmill (min)
60
40
20
0
veh
JQ1
B
Fractional shortening %
100
80
60
40
20
0
veh sham
JQ1 sham
NS
1
2
3
4
weeks
C
NS
Systolic BP (mmHg)
120
90
60
30
0
veh
JQ1
LVIDd (mm2)
20
10
0
NS
1
2
3
4
weeks
D
NS
Transaortic ΔP (mm Hg)
80
60
40
20
0
veh TAC
JQ1 TAC
(IVS + PW)d (mm)
1.8
1.4
1.0
NS
1
2
3
4
weeks

Figure S3 (related to Figure 3). JQ1 is well tolerated in mice and does not affect blood pressure or trans-aortic gradient. (A) Mice were given JQ1 (50 mg/kg/day IP) vs. vehicle for 17 days. Mice were subject to treadmill exercise (15 m/min, no incline) and time to exhaustion was measured (N=6). NS denotes statistical non-significance. (B) Echocardiographic parameters in sham treated mice (N=5). (C) Systolic blood pressure in mice treated with JQ1 (50 mg/kg/day IP) vs. vehicle for 17 days (N=5). (D) Pressure gradient across the surgically constricted segment of the aortic arch in mice 7 days after TAC (N=4). Data shown as mean ± SEM.

Figure S4

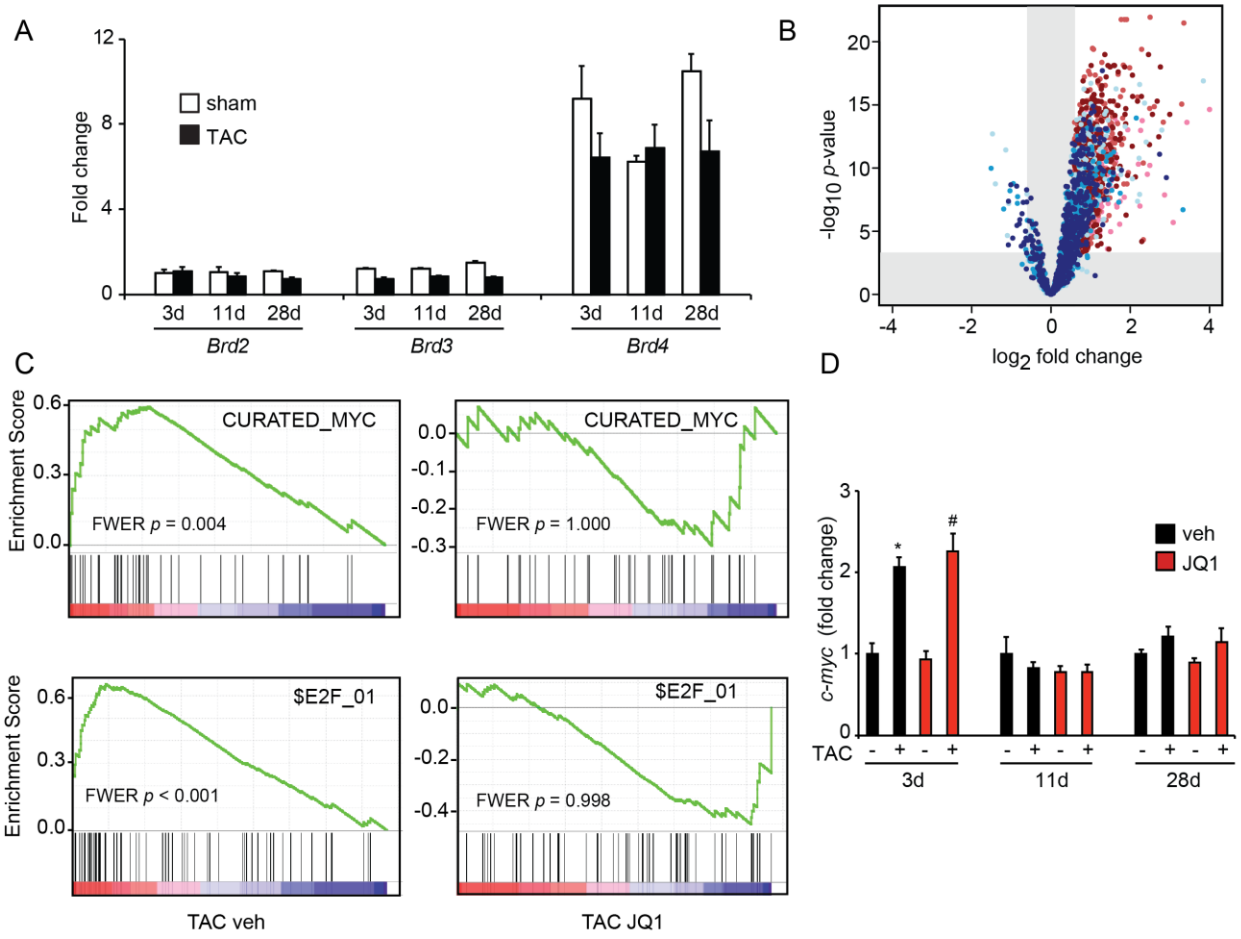

E

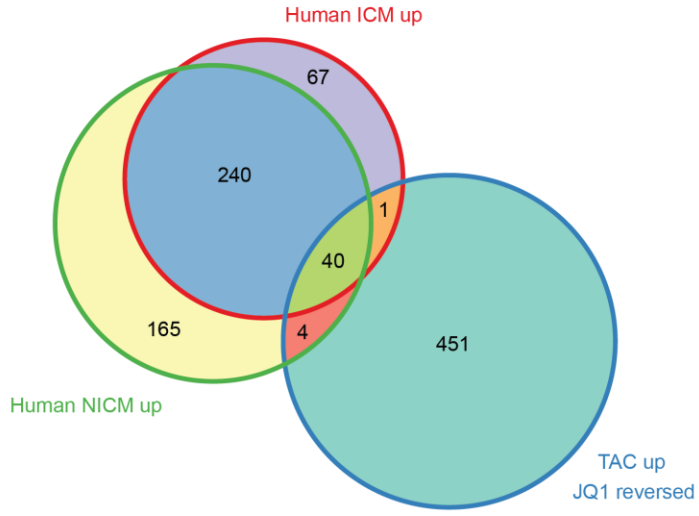

F

ALDH1A2	*LSP1*
ARHGAP15	*LTBP2*
ASPN	*LUM*
COL14A1	*MFAP4*
COL15A1	*MMP2*
COL1A1	*MXRA8*
COL1A2	*MYOF*
COL3A1	*NPPA*
COL6A1	*OLFML1*
CTSK	*OLFML3*
DIO2	*OMD*
DPYSL3	*PCOLCE*
ECM2	*PDGFC*
EFEMP2	*PHF11*
FBLN1	*PTN*
FBN1	*SFRP1*
FRZB	*SULF1*
IFIT3	*SVEP1*
ISLR	*THBS4*
ITIH5	*TSPAN6*

Figure S4 (related to Figure 5). Gene expression profiles of mouse hearts during TAC. (A) Relative expression of *Brd2-4* by qRT-PCR in mouse hearts after sham/TAC at indicated time-points (N=5-7). (B) Volcano plot showing fold change (x-axis) effect of TAC+JQ1 versus sham-veh (shades of blue) on all genes upregulated at any time-point by TAC. (i.e. TAC-vehicle versus sham-vehicle; shades of red). Progression from lighter to darker shading represents increasing time (3d, 11d, 28d). (C) GSEA showing upregulation of c-Myc and E2F signatures with TAC-veh but no statistically significant enrichment with JQ1 effect. Representative enrichment plots shown for 3 day time-point. (D) qRT-PCR from hearts of mice at indicated time-points (N=5-7) shows that JQ1 does not suppress *c-myc* induction. *P<0.05 vs. sham veh. $^{\#}$P<0.05 vs. sham JQ1. (E) Venn diagram showing intersection of TAC-inducible genes that were suppressed by JQ1 against expression profile of genes upregulated in advanced non-ischemic and ischemic heart failure in humans (Hannenhalli et al., 2006). Targets of BETs in the mouse TAC model overlapped in a statistically significant manner with the set of genes induced in human heart failure ($\chi^2 < 2 \times 10^{-14}$). (F) Genes populating the intersection of all 3 sets are listed. Data shown as mean $\pm$ SEM.

Figure S5

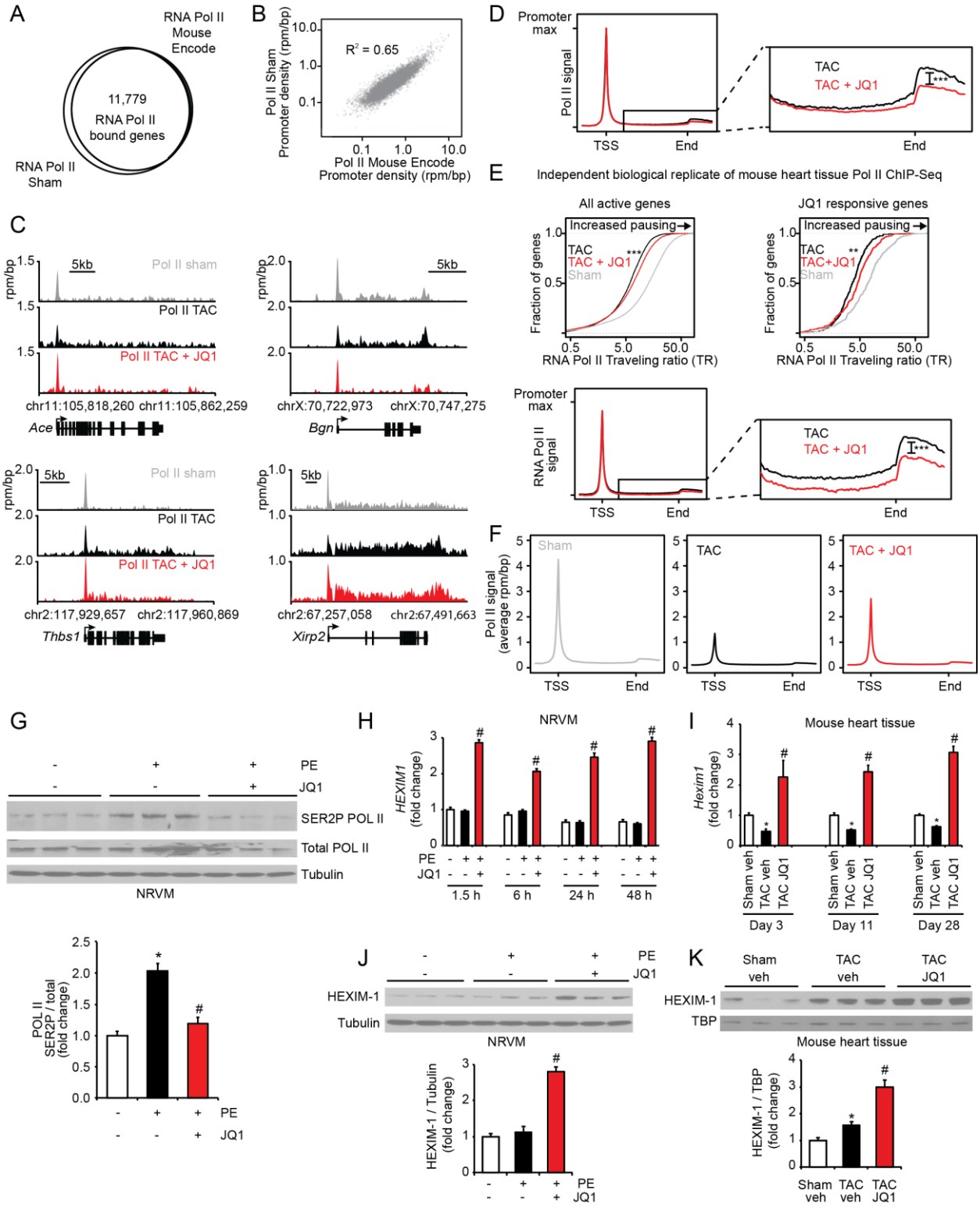
A
RNA Pol II Mouse Encode
11,779
RNA Pol II bound genes
RNA Pol II Sham
B
R² = 0.65
Pol II Sham Promoter density (rpm/bp)
Pol II Mouse Encode Promoter density (rpm/bp)
D
Promoter max
Pol II signal
TSS
End
TAC
TAC + JQ1
E
Independent biological replicate of mouse heart tissue Pol II ChIP-Seq
All active genes
JQ1 responsive genes
Increased pausing
Fraction of genes
RNA Pol II Traveling ratio (TR)
Sham
C
5kb
Pol II sham
Pol II TAC
Pol II TAC + JQ1
rpm/bp
chr11:105,818,260 chr11:105,862,259
Ace
chrX:70,722,973 chrX:70,747,275
Bgn
chr2:117,929,657 chr2:117,960,869
Thbs1
chr2:67,257,058 chr2:67,491,663
Xirp2
F
Sham
TAC
TAC + JQ1
Pol II signal (average rpm/bp)
G
PE
JQ1
SER2P POL II
Total POL II
Tubulin
NRVM
POL II SER2P / total (fold change)
H
NRVM
HEXIM1 (fold change)
1.5 h
6 h
24 h
48 h
I
Mouse heart tissue
Hexim1 (fold change)
Sham veh
TAC veh
TAC JQ1
Day 3
Day 11
Day 28
J
HEXIM-1
Tubulin
HEXIM-1 / Tubulin (fold change)
K
HEXIM-1
TBP
HEXIM-1 / TBP (fold change)

Figure S5 (related to Figure 6). BET bromodomains regulate pause release of RNA polymerase II and transcriptional elongation in the myocardium. (A) Venn diagram showing the overlap of transcriptionally active genes in either RNA Pol II sham treated heart (this study), or wild type heart (Mouse ENCODE) (Shen et al., 2012). A gene is defined as transcriptionally active if it contains an RNA Pol II enriched region within ±5kb of the transcription start site. (B) Scatter plot showing the average RNA Pol II promoter density in either sham treated (y-axis) or mouse ENCODE (x-axis) heart for genes that are transcriptionally active in either treatment condition. RNA Pol II average promoter density is displayed in units of rpm/bp. An R^2 correlation statistic is displayed. (C) Additional representative gene tracks showing ChIP-seq occupancy of RNA Pol II at *Ace*, *Bgn*, *Thbs1*, and *Xirp2* genes in sham treated (grey), TAC treated (black), or TAC + JQ1 treated (red) mouse heart. The x-axis shows genomic position. The y-axis shows ChIP-seq occupancy in units of rpm/bp. (D) Meta-gene representation of background subtracted RNA Pol II signal at genes that are transcriptionally active in either sham or TAC treated heart. The y-axis shows average RNA Pol II signal relative to the promoter max peak height for TAC (black) or TAC + JQ1 (red) treated heart. The x-axis shows a composite region comprised of the -3kb to transcription start site (TSS) region, the gene body, and transcription termination region (TTR) that spans +3kb from the gene end. The left panel shows the whole gene region while the right panel is a zoom of the gene body and TTR region. The difference in average RNA Pol II density in the gene body region and TTR region is statistically significant (*** designates Welch's two-tailed *t* test, $p < 2 \times 10^{-16}$). (E) Independent biologic replicate of RNA Pol II ChIP-seq in mouse hearts subject to sham, TAC, or TAC+JQ1 again demonstrates effect of JQ1 on suppressing TAC-induced transcriptional elongation in vivo. Empirical cumulative distribution plots of Pol II traveling ratios for genes that are transcriptionally active in either sham or TAC treated hearts (left) and genes that are TAC-induced and reversed by JQ1 (right). Differences in traveling ratio distribution between TAC and TAC+JQ1 treated hearts are statistically significant (*** Welch's two-tailed *t*

test, $p < 2 \times 10^{-16}$). Meta-gene representation of background subtracted RNA Pol II signal at genes that are transcriptionally active in either sham or TAC treated heart (bottom). The y-axis shows average RNA Pol II signal relative to the promoter max peak height for TAC (black) or TAC + JQ1 (red) treated heart. The x-axis shows a composite region comprised of the -3kb to transcription start site (TSS) region, the gene body, and transcription termination region (TTR) that spans +3kb from the gene end. The left panel shows the whole gene region while the right panel is a zoom of the gene body and TTR region. The difference in average RNA Pol II density in the gene body region and TTR region is statistically significant (*** designates Welch's two-tailed *t* test, $p < 2 \times 10^{-16}$). (F) Meta-gene representation of background subtracted RNA Pol II signal at genes that are transcriptionally active genes in either sham or TAC treated heart. The y-axis shows average RNA Pol II signal in units of rpm/bp for sham (grey, top), TAC (black, center) or TAC + JQ1 (red, bottom) treated heart. The x-axis shows a composite region comprised of the -3kb to transcription start site (TSS) region, the gene body, and transcription termination region (TTR) that spans +3kb from the gene end. (G) Western blots for Ser2P Pol II and Total Pol II from NRVM whole cell lysates. NRVM were treated with indicated combinations of JQ1 (500nM) and PE (100μM, 30min). Tubulin serves as additional loading control. Densitometric analysis (Ser2P/Total RNA Pol II) on bottom (N=3; *P<0.05 vs. untreated; $^{\#}$P<0.05 vs. PE alone). qRT-PCR for *HEXIM1* mRNA in (H) NRVM after indicated treatments/time-points (500nM JQ1; 100μM PE; N=4; $^{\#}$P<0.05 vs. PE alone) and (I) mouse heart tissue after sham, TAC, or TAC + JQ1 (N=5-7; *P<0.05 vs. sham veh; $^{\#}$P<0.05 vs. TAC veh). (J) HEXIM1 Western blot in NRVM whole cell lysates after indicated treatments (500nM JQ1; 100μM PE, 30min) with densitometry below (N=3; $^{\#}$P<0.05 vs. PE alone). (K) HEXIM1 Western blot from mouse heart tissue nuclear protein at 3-day postoperative time-point with densitometry below (N=3; *P<0.05 vs. sham veh; $^{\#}$P<0.05 vs. TAC veh). TBP serves as nuclear protein loading control. Data shown as mean ± SEM.

SUPPELMENTAL TABLES

Table S1 (related to Figure 2). Differential gene expression in NRVM. Excel file listing differential gene expression in NRVM treated with PE and JQ1 as indicated.

Table S2 (related to Figure 5). Differential gene expression in mouse hearts. Excel file listing differential gene expression in mouse hearts after sham, TAC, and TAC + JQ1 at indicated time-points.

Table S3 (related to Figure 6). ChIP-seq datasets. Excel file containing GEO accession number and background used for each dataset.

SUPPELMENTAL VIDEOS

Supplemental Video 1-2 (related to Figure 3). Representative high-resolution 2D echocardiographic images (parasternal short axis, mid-papillary level) from mice after 4 weeks TAC treated with vehicle (Video S1) vs. JQ1 (Video S2).

Supplemental Video 3-4 (related to Figure 3). Movie clip of mice in home cages (N=3) after 5 days of TAC that have received vehicle (Video S3) or JQ1 (Video S4) injections. The JQ1 treated mice are healthy appearing.

SUPPLEMENTAL EXPERIMENTAL PROCEDURES

Preparation of JQ1. JQ1 was synthesized and purified in the laboratory of Dr. James Bradner (DFCI) as previously published (Filippakopoulos et al., 2010). For in vivo experiments, a stock solution (50 mg/mL in DMSO) was diluted to a working concentration of 5 mg/mL in aqueous carrier (10% hydroxypropyl β-cyclodextrin; Sigma C0926) using vigorous vortexing. Mice were injected at a dose of 50 mg/kg given intraperitoneally once daily. Vehicle controls were given an equal amount of DMSO in carrier solution. All solutions were prepared and administered using sterile technique. For in vitro experiments, JQ1 and other BET inhibitors were dissolved in DMSO and administered to cells at indicated concentrations using an equal volume of DMSO as control. I-BET, I-BET-151, RVX-208, and PFI-1 were synthesized and purified in the laboratory of Dr. James Bradner.

Transverse aortic constriction and chronic PE infusion in mice. All mice were C57Bl/6J littermate males aged 10-12 weeks. For TAC, mice were anesthetized with ketamine/xylazine, mechanically ventilated (Harvard apparatus), and subject to thoracotomy. The aortic arch was constricted between the left and right carotid arteries using a 7.0 silk suture and a 27-guage needle as previously described (Hu et al., 2003). In our hands, this protocol created a consistent peak pressure gradient of approximately 50 mmHg across the constricted portion of the aorta. For PE infusion, mice were anesthetized using continuous 1% inhalational isofluorane. Mini-osmotic pumps (Alzet 2004, Durect Corp.) were filled with phenylephrine hydrochloride (PE, Sigma P8155) or vehicle (normal saline) and implanted subcutaneously on the dorsal aspect of the mouse. PE was infused at a dose of 75 mg/kg/day for 17 days. Injections of JQ1 or vehicle were begun 1.5 days postoperatively.

Echocardiography, blood pressure, and endurance exercise capacity measurements. For transthoracic echocardiography, mice were anesthetized with 1% inhalational isofluorane and

imaged using the Vevo 770 High Resolution Imaging System (Visual Sonics, Inc.) and the RMV-707B 30 MHz probe. Measurements were obtained from M-mode sampling and integrated EKV images taken in the LV short axis at the mid-papillary level (Haldar et al., 2010). Measurements of pressure gradients across the constricted portion of the aorta were obtained by high frequency Doppler as previously described (Liu et al., 2012). Conscious tail-vein systolic blood pressure was measured using the BP2000 Blood Pressure Analysis System (Visitech Systems, Inc.) as recommended by the manufacturer. To allow mice to adapt to the apparatus, we performed daily blood pressure measurements for one week prior to beginning experiments. Treadmill endurance exercise testing was performed on a motorized mouse treadmill (Columbus Instruments) as previously described (Haldar et al., 2012).

NRVM Culture. NRVM were isolated from the hearts of 2 day old Sprague-Dawley rat pups (Charles River) and maintained under standard conditions as described (Haldar et al., 2010). The cells were differentially pre-plated for 1.5h in cell culture dishes followed by 24h exposure to BrdU in culture medium to remove contaminating non-myocytes. Unless otherwise stated, NRVM were plated at a density of 10^5 cells/mL. Cells were initially plated in growth medium (DMEM supplemented with 5% FBS, 100 U/mL penicillin-streptomycin, and 2mM L-glutamine) for 24-36 hours and maintained in serum-free media thereafter (DMEM supplemented with 0.1% BSA, 1% insulin-transferrin-selenium liquid media supplement (Sigma I3146), 100 U/mL penicillin-streptomycin, and 2mM L-glutamine). Media was changed every 2-3 days. Prior to stimulation with agonists, NRVM were maintained in serum-free medium for 48-72 hours. For hypertrophic stimulation, NRVM were incubated with JQ1 versus DMSO at indicated concentrations for 6h followed by stimulation with PE (100μM) for indicated time-points.

NRVM BRD4 immunofluorescence. NRVM were grown on glass coverslips in 6-well dishes. Cells were fixed in PBS containing 3% PFA (15 min), permeabilized in PBST/0.25% Triton X-100 (10 min), and blocked in PBST/5% horse serum for 1h. Primary antibodies (anti sarcomeric

α-actinin, Sigma A7811, 1:800; anti-BRD4, Bethyl A301-985A, 1:250) were co-incubated in PBST/5% horse serum for 1h. Secondary antibodies (donkey α-mouse Alexa 594 red; donkey α-rabbit Alexa 488 green; Jackson Immuno-research) were co-incubated at 1:1000 each in PBST/5% horse serum for 1h. Coverslips were mounted onto glass slides with mounting media containing DAPI. Images were taken on a fluorescent microscope.

Cell area measurements. NRVM were plated on glass coverslips in 6-well dishes at a density of 10^5 cells/mL. After treatments, cells were briefly fixed in PBS containing 2% PFA, permeabilized with PBST/0.1% Triton X-100, and blocked in PBST/5% horse serum. Primary antibody was anti-sarcomeric α-actinin (Sigma A7811) at 1:800. Fluorophore-tagged anti-mouse secondary antibody (α-mouse Alexa 488 green) was used at 1:1000 dilution. Coverslips were mounted on glass slides with mounting media containing DAPI. Quantitation of cardiomyocyte cell surface area was performed on α-actinin-stained cardiomyocytes using fluorescent microscopy and NIH Image J software as previously described (Liang et al., 2001). Analysis consisted of at least 100 cardiomyocytes in 20–30 fields at 400x magnification. This process was replicated in a least three independent experiments, and the data were combined.

RNA purification and qRT-PCR. For tissue RNA, a 10-20 mg piece of mouse heart tissue was preserved in RNA Later stabilization reagent (Qiagen) followed by mechanical disruption/homogenization in PureZOL (BioRad) on a TissueLyser (Qiagen) using stainless steel beads (Qiagen). The aqueous phase was extracted with chloroform. RNA was purified from the aqueous phase using the Aurum purification kit (BioRad #732-6830) following manufacturer's instructions. For cellular samples, total RNA from NRVM was isolated using the High Pure RNA isolation kit (Roche #11828665001) with on-column DNAase treatment according to manufacturer's directions. Purified RNA was reverse transcribed to complementary DNA using the iScript™ RT Supermix (Biorad #170-8841) following manufacturer's protocol.

Quantitative real-time PCR was performed using TaqMan chemistry (Fast Start Universal Probe Master (Roche cat# 4914058001) and labeled probes from the Roche Universal Probe Library System) on a Roche LightCycler. Relative expression was calculated using the ΔΔCt-method with normalization to constitutive genes. NRVM data were normalized to *ACTB* (β-ACTIN). Mouse heart data were normalized to *Ppib* (Cyclophilin-B) Specific primer/probe sequences are available upon request.

Western blotting. For total cellular protein, cells were lysed in RIPA Buffer (Sigma R0278) supplemented with protease inhibitor (Roche cat#4693132001) and phosphatase inhibitor (Phos-STOP; Roche cat# 04 906 845 001) tablets. Nuclear protein was isolated using the NE-Per Kit (Thermo Scientific #78833) according to manufacturer's instructions. 20-40 μg of whole cell protein extracts or 20-50 μg of nuclear protein extracts were subject to SDS PAGE, transferred to nitrocellulose membranes, and Western blotting using the following antibodies: BRD4 (Bethyl #A301-985A), tubulin (Sigma T9026), RNA Polymerase II (Bethyl #A300 653A), Ser2P RNA Pol II (Abcam ab2478), Ser5P RNA Pol II (Abcam ab5131), HEXIM1 (Abcam ab25388), TBP (Abcam ab818).

Brd4 knockdown. For shRNA against mouse/rat *Brd4*, a specific hairpin sequence was subcloned into the pEQ adenoviral-shRNA vector (Welgen, Inc.). Recombinant adenoviruses for sh-*Brd4* and sh-control (scrambled shRNA) were amplified and purified by Welgen, Inc. NRVM were incubated with adenovirus (5-10 MOI) for 24 hours, followed by replacement of fresh serum-free media for another 24 hours. 48 hours after initial infection, cells were stimulated with PE.

Chromatin immunoprecipitation in NRVM. NRVM were plated in 15 cm dishes at 5 x 10^6 cells/dish. Chromatin pooled from approximately 15 x 10^6 NRVM was used for each immunoprecipitation. After indicated treatments, NRVM were fixed directly on the dish with 1%

formaldehyde for 10 minutes followed by quenching with 0.125M glycine for 5 minutes. Chromatin was extracted, followed by shearing on a BioRuptor (Diagenode; total 16 cycles, hi-power, 30sec on/off). The sonicated chromatin was immunoprecipitated with 5μg of antibody bound to Dynabeads (Invitrogen) followed by extensive washing and elution. Immunoprecipitate and input chromatin samples were then reverse cross-linked followed by purification of genomic DNA. Target and non-target regions of genomic DNA were amplified by qRT-PCR in both the immunoprecipitates and input samples using SYBR chemistry. Enrichment data were analyzed by calculating the immunoprecipitated DNA percentage of input DNA for each sample as previously described (Ott et al., 2012). Antibody used in ChIP was BRD4 (Bethyl #A301-985A). ChIP-PCR primer sequences are available upon request.

Chromatin immunoprecipitation in mouse heart tissue. Mice were subject to sham or TAC surgery, followed by JQ1 (50 mg/kg/day IP) and vehicle administration beginning 1.5 days after surgery. On the fourth postoperative day, hearts were rapidly excised, finely minced in PBS supplemented with protease inhibitors, fixed in 1.1% formaldehyde in PBS for 10 minutes, and quenched by adding glycine to 0.125M final concentration for 5 minutes. Two adult mouse hearts were pooled to prepare a single chromatin sample. After crushing tissue in a Dounce homogenizer, chromatin was extracted, followed by shearing on a BioRuptor (Diagenode; total 40 cycles, hi-power, 30sec on/off). The sonicated chromatin was divided into thirds and each fraction was immunoprecipitated with 5μg of antibody bound to protein G conjugated Dynabeads (Invitrogen) followed by extensive washing and elution. Immunoprecipitate and input chromatin samples were then reverse cross-linked followed by purification of genomic DNA. Antibodies used in hear tissue ChIP were BRD4 (Bethyl #A301-985A) and RNA Polymerase II (Santa Cruz N-20, sc-899).

Illumina DNA Sequencing and Library Generation. Purified ChIP DNA was used to prepare Illumina multiplexed sequencing libraries. Libraries for Illumina sequencing were prepared

following the Illumina TruSeq™ DNA Sample Preparation v2 kit protocol with the following exceptions. After end-repair and A-tailing, immunoprecipitated DNA (~10-50ng) or whole cell extract DNA (50ng) was ligated to a 1:50 dilution of Illumina Adapter Oligo Mix assigning one of 24 unique indexes in the kit to each sample. Following ligation, libraries were amplified by 18 cycles of PCR using the HiFi NGS Library Amplification kit from KAPA Biosystems. Amplified libraries were then size-selected using a 2% gel cassette in the Pippin Prep™ system from Sage Science set to capture fragments between 200 and 400 bp. Libraries were quantified by qPCR using the KAPA Biosystems Illumina Library Quantification kit according to kit protocols. Libraries with distinct TruSeq indexes were multiplexed by mixing at equimolar ratios and running together in a lane on the Illumina HiSeq 2000 for 40 bases in single read mode.

ChIP-seq Data analysis

Accessing data generated in this manuscript. All ChIP-seq and expression data generated in this manuscript can be found online associated with GEO Accession ID GSE46668 (www.ncbi.nlm.nih.gov/geo/). Both sets of independent biologic replicates for ChIP-Seq experiments are deposited.

Gene sets and annotations. All analysis was performed using RefSeq (NCBI37/MM9) mouse gene annotations.

ChIP-seq data processing. All ChIP-seq datasets were aligned using Bowtie (version 0.12.9) (Langmead et al., 2009) to build version NCBI37/MM9 of the mouse genome. Alignments were performed using the following criteria: -n2, -e70, -m1, -k1, --best. These criteria preserved only reads that mapped uniquely to the genome with 1 or fewer mismatches.

Calculating read density. We calculated the normalized read density of a ChIP-seq dataset in any region as in (Lin et al., 2012). Briefly, ChIP-seq reads aligning to the region were extended by 200bp and the density of reads per basepair (bp) was calculated. Only positions with at least

2 overlapping extended reads contributed to the overall region density. The density of reads in each region was normalized to the total number of million mapped reads producing read density in units of reads per million mapped reads per bp (rpm/bp)

Identifying ChIP-seq enriched regions. We used the MACS version 1.4.2 (Model based analysis of ChIP-Seq) (Zhang et al., 2008) peak finding algorithm to identify regions of ChIP-seq enrichment over background. A p-value threshold of enrichment of 1e-9 was used for all datasets. The GEO accession number and background used for each dataset can be found in the accompanying supplementary file (Table S3).

Defining actively transcribed genes. In heart samples, a gene was defined as actively transcribed if enriched regions for RNA Polymerase II (RNA Pol II) were located within $\pm$ 5kb of the TSS.

Defining active enhancers. Active enhancers were defined as H3K27Ac regions outside of annotated transcription start sites using criteria established in (Loven et al., 2013).

Determination of RNA Pol II traveling ratio. We determined the ratio of background subtracted RNA Pol II ChIP-seq levels in initiating to elongating regions, a measure known as the traveling ratio (TR) (Rahl et al., 2010) in RNA Pol II heart samples (Figure 7F). We defined the initiating region as $\pm$ 300bp around the TSS. We defined the elongating region as +300bp from the TSS to +3,000bp after the gene end. The statistical significance of changes in the distribution of traveling ratios was determined using a Welch's two-tailed *t* test

Creating meta-gene representations of RNA Pol II occupancy. Meta-gene representations of RNA Pol II occupancy (Figure S5D) were determined by first binning each transcriptionally active gene in either TAC or Sham conditions into three regions: i) the upstream promoter - from 3kb upstream of the TSS to the TSS (50bp bins), ii) the gene body - from the TSS to the gene end (200 bins), iii) the transcription termination region (TTR) - from the gene end to +3kb

downstream (50bp bins). RNA Pol II density in each region was calculated and the average RNA Pol II density in that region was plotted relative to the maximum promoter density (Figure S5D) or plotted in units of average rpm/bp. The difference in relative RNA Pol II density in the gene body and TTR region was found to be statistically significant using a Welch's two-tailed *t* test.

Histological analysis. Short-axis heart sections from the mid-ventricle were fixed in PBS/4% paraformaldehyde and embedded in paraffin. Cardiomyocyte cross sectional area was determined by staining with rhodamine-conjugated wheat-germ agglutinin (Vector Laboratories RL-1022) as quantified as previously described (Froese et al., 2011). Fibrosis was visualized using Masson's Trichrome staining kit (Biocare medical) with quantification of fibrotic area as previously described (Song et al., 2010). Terminal deoxynucleotidyl transferase dUTP nick-end label (TUNEL) staining and quantification was performed as previously described (Song et al., 2010) using the ApopTag Plus kit (Millipore) according to manufacturer's instructions. Myocardial capillary staining was performed in frozen LV sections using anti-PECAM-1 antibodies (EMD Millipore cat# CBL-1337) as previously described (Haldar et al., 2010).

Gene expression microarray and bioinformatic analyses. RNA was hybridized to Affymetrix Mouse Gene 1.0 ST or Rat Genome 230 2.0 arrays, as appropriate, per standard protocol at the DFCI Mircoarray Core. Bioconductor (http://bioconductor.org) packages *affyQCReport*, *rma*, and *limma* were used to perform quality control, normalization and differential expression analysis, respectively. Genes with a fold-change of >1.5 and Benjamini-Hochberg adjusted P-value < 0.05 were considered significant. Dynamic changes in differentially expressed genes were visualized with the Gene Expression Dynamics Inspector (GEDI, version 2.1) (Eichler et al., 2003). Lists of up- and down-regulated genes were submitted online to the DAVID server (david.abcc.ncifcrf.gov) for functional annotation. For gene set enrichment analysis (GSEA), collections of gene signatures were downloaded from the Molecular Signatures Database

(MSigDB, http://www.broadinstitute.org/gsea/msigdb) and supplemented with manually curated signatures derived from published reports. GSEA was performed on log_2-converted expression values using the T-test metric. Genes significantly up-regulated in human ICM or NICM were taken from Supplemental Table 1 of Hannenhalli *et al*. (Hannenhalli et al., 2006) and converted to their mouse homologs using the HomoloGene database (http://www.ncbi.nlm.nih.gov/homologene). To test for significant overlap of these human gene sets with genes induced by TAC and reversed by JQ1, we considered only homologous genes represented on the mouse arrays.

SUPPLEMENTAL REFERENCES

Froese, N., Kattih, B., Breitbart, A., Grund, A., Geffers, R., Molkentin, J.D., Kispert, A., Wollert, K.C., Drexler, H., and Heineke, J. (2011). GATA6 promotes angiogenic function and survival in endothelial cells by suppression of autocrine transforming growth factor beta/activin receptor-like kinase 5 signaling. J Biol Chem *286*, 5680-5690.

Haldar, S.M., Jeyaraj, D., Anand, P., Zhu, H., Lu, Y., Prosdocimo, D.A., Eapen, B., Kawanami, D., Okutsu, M., Brotto, L.*, et al.* (2012). Kruppel-like factor 15 regulates skeletal muscle lipid flux and exercise adaptation. Proc Natl Acad Sci U S A *109*, 6739-6744.

Haldar, S.M., Lu, Y., Jeyaraj, D., Kawanami, D., Cui, Y., Eapen, S.J., Hao, C., Li, Y., Doughman, Y.Q., Watanabe, M.*, et al.* (2010). Klf15 deficiency is a molecular link between heart failure and aortic aneurysm formation. Science translational medicine *2*, 26ra26.

Hu, P., Zhang, D., Swenson, L., Chakrabarti, G., Abel, E.D., and Litwin, S.E. (2003). Minimally invasive aortic banding in mice: effects of altered cardiomyocyte insulin signaling during pressure overload. Am J Physiol Heart Circ Physiol *285*, H1261-1269.

Langmead, B., Trapnell, C., Pop, M., and Salzberg, S.L. (2009). Ultrafast and memory-efficient alignment of short DNA sequences to the human genome. Genome biology *10*, R25.

Liang, Q., De Windt, L.J., Witt, S.A., Kimball, T.R., Markham, B.E., and Molkentin, J.D. (2001). The transcription factors GATA4 and GATA6 regulate cardiomyocyte hypertrophy in vitro and in vivo. J Biol Chem *276*, 30245-30253.

Liu, Q., Chen, Y., Auger-Messier, M., and Molkentin, J.D. (2012). Interaction between NFkappaB and NFAT coordinates cardiac hypertrophy and pathological remodeling. Circ Res *110*, 1077-1086.

Ott, C.J., Kopp, N., Bird, L., Paranal, R.M., Qi, J., Bowman, T., Rodig, S.J., Kung, A.L., Bradner, J.E., and Weinstock, D.M. (2012). BET bromodomain inhibition targets both c-MYC and IL7R in high-risk acute lymphoblastic leukemia. Blood *120*, 2843-2852.

Zhang, Y., Liu, T., Meyer, C.A., Eeckhoute, J., Johnson, D.S., Bernstein, B.E., Nusbaum, C., Myers, R.M., Brown, M., Li, W.*, et al.* (2008). Model-based analysis of ChIP-Seq (MACS). Genome biology *9*, R137.